D Synthesis

In this chapter, I aim at a joint interpretation of the results obtained in this study by seismic and petrological investigations, and to discuss these results together with results from different previous geoscientific studies in the area (including seismicity, gas-geochemistry, and seismic studies). Finally, a process-orientated model of the system crust-uppermost mantle beneath the earthquake swarm region and intraplate CO_2 degassing field is presented.

D.1 A seismic and petrologic model of the crust-mantle transition and the origin of the "6 s phase"

To relate results from seismic studies to petrology, it is necessary to compare seismic velocity-depth profiles with velocity values of regionally occurring rocks, which can be measured on hand specimen in the laboratory or calculated from the modal (mineral) composition of rocks [e.g., *O'Reilly et al.,* 1990; *James et al.,* 2004]. Unfortunately, the xenoliths from Mýtina are too small to measure seismic velocities directly. So, the elastic properties can only be estimated comparing the xenoliths to published data of rock samples of similar mineralogy or by calculation from the modal composition. Pressure estimates on xenoliths and temperatures from geotherms can be used to correct the elastic parameters (seismic velocities) for conditions in their primary depth in the lower crust or uppermost mantle (at the crust-mantle boundary). In Figure D.1 the results from the receiver function study and the petrologic and geobarometric studies on xenoliths from the Mýtina tephra are combined.

D.1.1 Relating seismic velocities to petrology

D.1.1.1 Upper and middle crust

Regional P-wave seismic velocity models published in literature (see Figure B.9) let me argue that most of the upper and middle crust is composed of meta-sedimentary, granitic, and granulitic rocks comparable to rocks at the surface in the western and northern Bohemian Massif. This concurs with the petrophysical interpretation of the MVE90 and GRANU95 seismic profiles by *Mueller* [1995], *DEKORP and Orogenic Processes Working Groups* [1999], and *Krawczyk et al.* [2000]. Further arguments come from the KTB deep drill hole where similar rocks were cored down to nine kilometres [*Emmermann and Lauterjung,* 1997], which is one third of the crustal thickness in the region. Seismic velocities of typical crustal rocks are compiled by *Christensen and Money* [1995] and *Rudnick and Fountain* [1995].

D.1.1.2 Lower crust and uppermost mantle

Laboratory elastic parameter (seismic velocity) studies for lower crust and upper mantle rocks are rare, especially for hydrous mantle minerals. Previous compilations of elastic parameters and their dependence on pressure and temperature conditions valid for the crust-mantle boundary were published, e.g., by *Christensen* [1989] and *Mechie et al.* [1994b]. More recently, compilations were published by *Shaocheng Ji et al.* [2002] and *Hacker and Abers* [2004]. However, some of the necessary mineral elastic parameters were still calculated from similar minerals instead of directly measured [see *Hacker and Abers*, 2004]. To get an idea of probable seismic velocities in the upper mantle of the study area, seismic velocities of hypothetic rocks similar to the analysed ultramafic nodules (Table D.I) were calculated using the Excel-workbook provided by *Hacker and Abers* [2004]. The results using this workbook are similar to the velocity calculations using the elastic parameter values given by *Mechie et al.* [1994b] (see Appendix D.i).

At pressure-temperature conditions at the crust-mantle boundary (1.0 GPa, 650°C; extrapolation of the CT-geotherm published by *Čermák* [1994]) clinopyroxenites (v_s 4.2 km/s, v_p 7.5 km/s) and hornblendites (v_s 4 km/s, v_p 7.1 km/s) have 5 to 12 % lower seismic velocities than spinel lherzolites (v_s 4.6 km/s, v_p 8.1 km/s). Wehrlites have 2 to 3 % lower seismic velocities (v_s 4.5 km/s, v_p 7.9 km/s). Assuming lower temperatures (550°C), seismic velocities would increase by 0.05 km/s. At 2.0 GPa and 1000°C (extrapolation of the CT-geotherm published by *Čermák* [1994]) seismic velocities are reduced by about 0.1 km/s in comparison to the values at 1.0 GPa and 650°C. For the noritic sample seismic velocities were calculated at 0.6 GPa and 600°C (v_s 3.8 km/s, v_p 6.8 km/s).

D.1.2 The origin of the “6 s phase”

Considering all available information, it is possible to discuss the origin of the observed “6 s phase” in the receiver function study. As it is evident from receiver function modelling (Figures B.15, D.1) the origin of the “6 s phase” could be in the crust or mantle or both. As it is already mentioned above, no further move-out with epicentral distance can be observed; indicating that this converted phase might be of upper mantle origin. The independent observation of the converter at the same location at different stations (coherent stacking at upper mantle depths) may also be an argument for this interpretation. However, from the receiver functions alone I cannot favour model b or model e (Figure B.15b, e) at the moment. Both might be geological reasonable and fit the observed data very well.

Table D.I. Seismic velocities for hypothetic mantle assemblages beneath the swarm-earthquake region Vogtland/NW-Bohemia at specified pressure and temperature conditions. Temperatures of about 650°C near the Moho (1 GPa) and 1000°C at 2 GPa were assumed, according to the extrapolation of the CT-geotherm published by *Čermák* [1994]. The composition of the selected rocks is close to the composition of the ultramafic nodules analysed in this study.
For the calculation the Excel-workbook of *Hacker and Abers* [2004] was used. Parameters for minerals were calculated from the mineral end-member values.

vol.%	norite	hbl-ite	cpx-hbl-ite	cpx-ite	wehrlite		hbl-peridotite			sp-lherzolite 1		sp-lherzolite 2		dunite		pyrolite	harzburgite	lhz W	eclogite
alpha quartz																			6.0
high albite	24.0																		
anorthite	31.0																		
orthoclase																			
sanidine																			
almandine																2.1	0.7	5.2	18.0
grossular																1.1	0.5	2.2	13.0
pyrope																10.8	5.4	14.3	11.0
forsterite					44.5	44.5	49.8	49.8	49.8	60.0	60.0	76.0	76.0	91.0	91.0	54.5	61.7	51.4	
fayalite					5.0	5.0	10.2	10.2	10.2	6.0	6.0	8.0	8.0	9.0	9.0	6.7	5.4	5.7	
enstatite	26.3									16.4	16.4	9.6	9.6			14.7	16.8	1.1	
ferrosilite	10.2									1.6	1.6	1.0	1.0			1.5	1.6	0.1	4.0
diopside	6.3		36.0	75.0	44.1	44.1	8.2	8.2	8.2	13.7	13.7	4.6	4.6			7.4	6.7	18.0	24.0
hedenbergite	1.8		12.0	25.0	5.5	5.5	1.8	1.8	1.8	1.4	1.4	0.4	0.4					2.0	2.0
jadeite																1.2	1.2		18.0
pargasite		100.0	47.0				25.0	25.0	25.0										
phlogopite	0.5		3.0																
muscovite																			2.0
spinel					1.0	1.0	5.0	5.0	5.0	1.0	1.0	0.5	0.5						2.0
hercynite																			
magnetite			2.0																
Sum	100.0	100.0	100.0	100.0	100.0	100.0	100.0	100.0	100.0	100.0	100.0	100.0	100.0	100.0	100.0	100.0	100.0	100.0	100.0
p (GPa)	0.6	1.0	1.0	1.0	1.0	2.0	1.0	1.5	2.0	1.0	2.0	1.0	2.0	1.0	2.0	2.0	2.0	2.0	1.0
T (°C)	600	650	650	650	650	1000	650	800	1000	650	1000	650	1000	650	1000	1000	1000	1000	650
Physical properties calculated with Hashin-Shtrikman average:																			
H_2O (wt%)	0.0	2.2	1.2	0.0	0.0	0.0	0.6	0.6	0.6	0.0	0.0	0.0	0.0	0.0	0.0	0.0	0.0	0.0	0.1
rho (g/cm3)	3.0	3.1	3.2	3.3	3.3	3.3	3.3	3.3	3.3	3.3	3.3	3.3	3.3	3.3	3.3	3.3	3.3	3.4	3.5
V_p (km/s)	6.77	7.12	7.23	7.52	7.87	7.77	7.79	7.76	7.70	7.98	7.86	8.07	7.96	8.17	8.07	7.99	7.97	8.06	7.95
V_s (km/s)	3.75	4.01	4.04	4.19	4.45	4.35	4.40	4.36	4.30	4.57	4.46	4.62	4.51	4.67	4.56	4.52	4.53	4.52	4.53
K (GPa)	81	89	98	110	117	115	115	115	114	117	116	121	119	124	122	122	119	127	126
G (GPa)	42	49	52	58	65	62	64	63	61	69	65	70	67	72	68	68	67	69	72
Poissons	0.28	0.27	0.27	0.28	0.27	0.27	0.27	0.27	0.27	0.26	0.26	0.26	0.26	0.26	0.26	0.27	0.26	0.27	0.26
v_p/v_s	1.80	1.78	1.79	1.80	1.77	1.79	1.77	1.78	1.79	1.75	1.76	1.75	1.77	1.75	1.77	1.77	1.76	1.78	1.75

D.1.2.1 Arguments for an upper mantle origin of the “6 s phase”

Further indications for local seismic discontinuities in the uppermost mantle beneath the Vogtland/NW-Bohemia region came from reflection seismic profiling. *Tomek et al.* [1997] detected three mantle reflectors (MR) at depths of 35 (MR_1), 42 (MR_2, box P in Figure B.14a), and 56 km (MR_3, box L in Figure B.14a) along the 9HR seismic profile (see Figure A.5). Reflector M_1 at about 32 km depth could also be interpreted to be of subcrustal origin. Unfortunately, it is not possible to interpret polarities of these reflections [*Tomek*, personal communication]. Reflection MR_3 argues for a local sharp discontinuity in the uppermost mantle instead of the gradient zone modelled in Figure B.15e. In case of a very local discontinuity no multiple converted phases could be observed.

Subcrustal lithospheric seismic discontinuities were previously found worldwide in a wide variety of tectonic settings [cf., *Hales*, 1969; *Ginzburg et al.,* 1979; *Keller et al.,* 1994; *Bostock*, 1999; *Ascencio et al.,* 2003; *Rost and Williams,* 2003]. Discussed causes of such discontinuities include spinel-to-garnet transition, compositional differences due to differentiation processes or the presence of partial melt, anisotropic layers with preferred orientation of olivine crystals, and relic subduction zone eclogitized oceanic crust.

Assuming that model e explains the ”6 s phase”, the piercing points of the analysed rays at 50 km depth were plotted (Figures B.14a, 15e) together with the results of the gas mapping of *Weinlich et al.* [1999] (see Figure A.4a). Interpreting the “6 s phase” as being of uppermost mantle origin, the distribution of red points in Figure B.14a marks more or less the areas with relatively reduced seismic velocities in the uppermost mantle above a converter. If the “6 s phase” is associated with upper mantle structure the average velocity reduction in the uppermost mantle above the converter might be up to 8 % (v_p/v_s = 1.79) or 5 % for v_p and 11.5 % for v_s (v_p/v_s = 1.92), respectively, relative to a “normal” upper mantle P-wave velocity of 8.0 km/s (v_p/v_s = 1.79). This could indicate the presence of 3 to 5 % melt or fluids in the uppermost mantle [according to *Faul et al.,* 1994]. Even less melt might be present using the values for velocity reduction obtained by *Hammond and Humphreys* [2000].
As discussed by *Glahn et al.* [1992], water-bearing minerals like phlogopite and amphibole can lower the seismic velocities in the uppermost mantle significantly. Up to now, orthopyroxene-bearing xenoliths could not be found in the Quaternary volcanics of the investigated area. The most common mantle xenoliths are wehrlites and clinopyroxenites characterizing the uppermost mantle beneath the study area as metasomatic. Some of them contain also significant amounts of amphibole. These rock types can have more than 5 % lower seismic velocities than normal upper mantle rocks lherzolitic-harzburgitic in composition (see Table D.I). This could explain at least some of the assumed velocity reduction. The higher seismic velocities beneath the discontinuity might represent “normal” upper mantle rocks or slightly depleted rocks (harzburgites/dunites) in the source region of alkaline magmas.

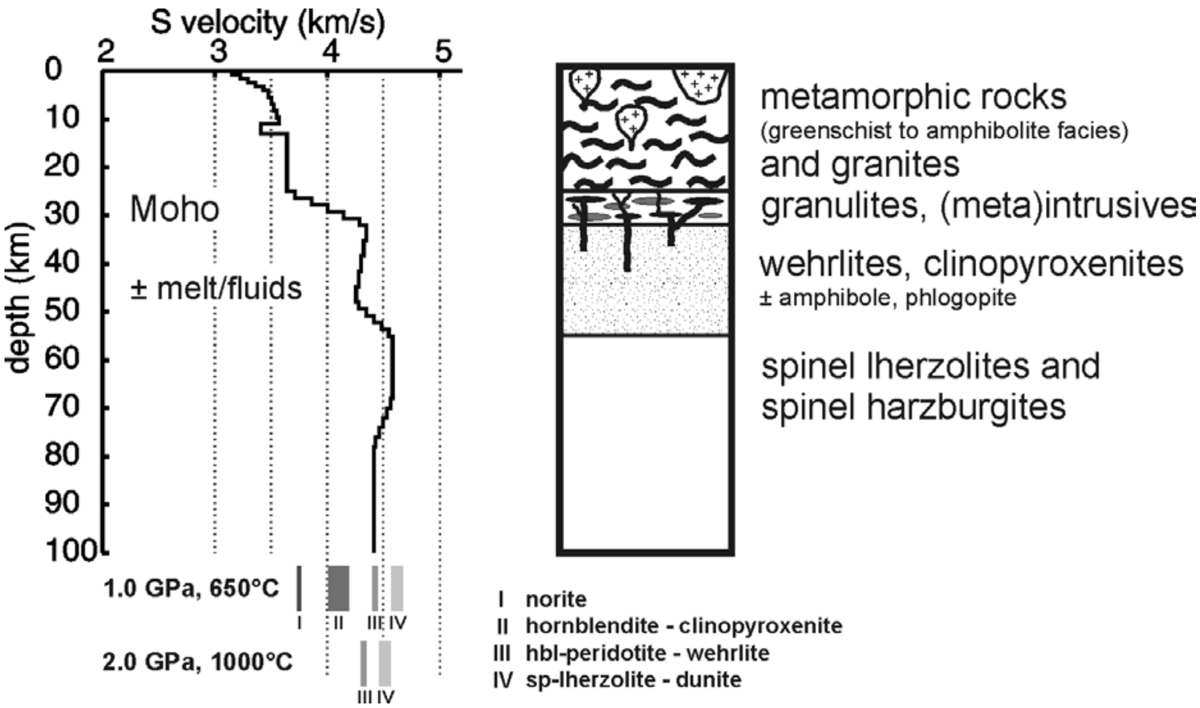

Figure D.1
Model of the Pleistocene lithosphere beneath the Železná Hůrka area. Left: Proposed present-day shear wave velocity model beneath NW-Bohemia for the area of the "6 s phase" (see Figure B.14). Also shown are the ranges of shear wave velocities for different (ultra-) mafic rock types at different temperature-pressure conditions. Temperatures of about 650°C near the Moho (1 GPa) and 1000°C at 2 GPa were assumed, according to the extrapolation of the CT-geotherm published by *Čermák* [1994]. For the calculation of the seismic velocities of rocks the Excel-workbook of *Hacker and Abers* [2004] was used (see Table D.I).
It should be pointed out, that it is not possible to derive true velocity-depth profiles using receiver functions alone, however the velocity difference across seismic discontinuities is more or less well resolved. Therefore, the comparison of the velocity-depth profile and the shear wave velocities calculated for different rock types should not be over-interpreted.
Right: Petrological crustal section derived from the xenolith study and local surface geology.

The assumption on the presence of partial melts in the uppermost mantle above the converter concur with the observed isotope signatures of the CO_2-dominated gas exhalations in the western Eger Rift [*Weinlich et al.,* 1999]. The gas escape centres with helium isotope signatures of the subcontinental lithospheric mantle ($^3He/^4He$ ratios up to 5.9 Ra in the Cheb Basin) [*Bräuer et al.,* 2004] as well as the position of the Quaternary scoria cones of Komorní Hůrka and Železná Hůrka overlap with the position of the local converter/reflector in the depth of approximately 50 to 60 km (Figures A.5, B.14) [see also *Tomek et al.,* 1997].

The observed seismic converter/reflector at about 50 to 60 km depth might also be explained as related to the spinel lherzolite-garnet lherzolite transition as discussed by *O'Reilly and Griffin* [1985] for the uppermost mantle of southeastern Australia. Further constraints for a sharp seismic discontinuity in that depth range came from a study of *Webb and Wood* [1986], who showed that the transition might occur over a pressure interval of only about 2 kbar (6 km). However, up to now no garnet-bearing upper mantle xenoliths are reported from the Eger Rift area and the spinel stability field might be expanded down to about 90 km [*Franz et al.,* 1997; *Medaris et al.,* 1999]. Therefore, I favour the interpretation that the seismic discontinuity is related to the base of a metasomatic uppermost mantle containing a few percent of melts.

As mentioned above, seismic discontinuities in the uppermost mantle could be related to the boundary between two layers with differently orientated seismic anisotropy. Seismic anisotropy in the upper mantle is indicated by SKS and P residua studies [e.g., *Bormann et al.,* 1996; *Plenefisch et al.,* 2001; *Babuška and Plomerová*, 2001]. But the observation of the „6 s phase“ does not show clear dependence on the back-azimuth of analysed events. Also no coherent signals in the T-components could be identified in the present dataset. Such signals would indicate anisotropic seismic properties in the studied depth interval. Possibly, the existence of anisotropic layers could be proved or disproved with a more extended database [see also *Christensen et al.,* 2001].

Finally, the observed conversions might be caused by eclogites, representing material possibly subducted during the Variscan convergence. But up to now no eclogite xenoliths could be identified, but the possibility of their existence cannot be ruled out definitively. Further detailed studies on the lateral extension and possible depth variations of the converter/reflector might help to solve this question.

D.1.2.2 Arguments for a crustal origin of the “6 s phase”

There are also arguments for a possible discontinuity at the base of the upper crust (model in Figure B.15b). The nature of the seismicity in the investigated area indicates a fluid-rich seismogenic crust. The earthquake swarms are commonly interpreted as fluid-triggered seismicity [*Špičak et al.*, 1999; *Dahm et al.*, 2000; *Špičak and Horálek,* 2001; *Horálek et al.*, 2002; *Plenefisch et al.*, 2003; *Vavryčuk*, 2002; *Fischer and Horálek,* 2003]. *Weise et al.* [2001] calculated the CO_2 volume of crustal origin, released by seismically induced micro-fracturing in December 1994 to be between 9.3 x 10^{10} and 0.1 x 10^{10} l. Fluid traps in the seismogenic upper crust are of local dimension and possibly spot-like distributed [*Behr et al.*, 1994; *Boušková et al.*, 2003; *Parotidis et al.*, 2003]. Furthermore, the rareness of CO_2 exhalations directly in the epicentral area of Nový Kostel could be explained with permeability barriers, capping the hydraulic system. Mantle-derived fluids may be trapped in the crustal segment below such a barrier [*Bräuer et al.*, 2003].

Because of geochemical evidences and indications from reflection seismic profiling, a combination of both velocity models b and e with half the amplitudes of each anomalous layer might also be plausible (Figures B.15f, D.1).

D.2 The structure of the crust and the subcrustal mantle beneath the western Eger (Ohře) Rift – towards a process orientated model

The observed anomaly at the Moho level and the local indications for a seismic converter/reflector at about 50 to 60 km depth concur with the distribution of the CO_2 emanation centres and the Quaternary volcanoes at the surface, as well as with the main swarm-earthquake activity in the upper crust of the Vogtland/NW-Bohemia area. Therefore, I believe that all these observations are somehow interrelated by an active zone of mantle melting and magmatic underplating, associated with recent extensional tectonics, which may be illustrated by Figure D.2.

The helium isotopic signature of several CO_2 vents at the surface reaches up to 5.9 Ra. This is an evidence for the origin of the CO_2-dominated gas phase from subcontinental lithospheric mantle (SCLM) according to *Gautheron and Moreira* [2002] and *Bräuer et al.* [2004]. CO_2 and other volatile components (e.g. Ar, H_2O, N_2, Ne) are included in the partial melting process of the upper mantle (at approximately 90 to 100 km depth). There need to be no difference between transport of the CO_2 (and other volatiles) and the magma transport in the upper mantle. *Weinlich et al.* [1999] evaluated the composition of the magmas in the uppermost mantle of the working area and calculated the magmatically dissolved CO_2 portion. Results of thermobarometric studies on melt and carbon dioxide inclusions in Saxon Tertiary alkalibasaltic volcanics and peridotite xenoliths [*Thomas*, 1992] argues, that the formation of a CO_2-dominated gas phase (the separation of CO_2 from the melt) starts in the depth range of 30 to 21 km. Further studies on fluid inclusions in upper mantle derived rocks indicate that a free gas phase can exist at least up to 1.2 to 1.4 kbar and maybe down to 70 km [cf., *Pasteris,* 1987; *Andersen and Neumann,* 2001]. So I conclude, CO_2 with SCLM-signature at surface is directly linked to magmatic processes and the melt reservoir(s) in the uppermost mantle, or as discussed above to metasomatic processes in the uppermost mantle (also related to alkaline magmatism).

The structural (seismic) and petrological (xenoliths) results of this study in combination with the geochemical and isotope evidence from previous investigations enable to find a link for mantle-crust interaction processes at different depths (Figure D.2). From bottom to top I try to relate a number of features to presently active magmatic underplating processes overprinting the Cainozoic Eger Rift environment.

Asthenospheric up-welling beneath the western Eger Rift area is indicated by different studies [*Rajkes and Bonjer,* 1983; *Faber et al.,* 1986; *Plomerová and Babuška,* 1988; *Plešinger et al., 1994; Passier and Snieder;* 1996; *Plomerová et al.,* 1998; *Babuška and Plomerová,* 2001]. An **isolated subcrustal seismic converter/reflector** exists at a depth of approximately 50 to 60 km ["6 s phase", *this study*; *Tomek et al.,* 1997], which can be interpreted as the base of a zone of a highly metasomatic mantle (containing wehrlites, clinopyroxenites, amphibole-peridotites) infiltrated by melts (magma/fluid reservoirs). Besides that, the position of a **local scale Moho updoming** from about 31 in the surroundings to 27 km in the centre (NNW-SSE extension of 40 km) overlaps with a presently active **CO_2 mantle-degassing field** showing clear upper mantle derived helium portions [*Weinlich et al.,* 1999, 2003; *Geissler et al.,* 2004a]. Decreased sub-Moho P-wave velocities of 7.6 to 7.7 km/s [*Giese,* 1976; *Hemmann,* 2002; *Hemmann et al.,* 2003] together with local observations of **weak or absent Moho conversions** [*this study*] point to a complex transition zone rather than a sharp velocity contrast at the crust-mantle boundary. Thermal and magmatic overprinting of the crust-mantle boundary in this region with small intrusions into the lower crust might cause a locally complex and broad Moho transition zone. As it is assumed by different authors [e.g., *McKenzie*, 1984; *Furlong and Fountain*, 1986; *Mengel and Kern*, 1991], the crust-mantle boundary acts as a barrier for ascending mafic magmas (ponding region). I suppose, the observed seismic Moho beneath the region is a relatively young feature. **Increased reflectivity in the lower crust** northeast of the KTB and beneath the Vogtland area [*Trappe and Wever,* 1990; *Behr et al.,* 1994; *Bleibinhaus et al.,* 2003] may be interpreted as low angle shear zones partly filled with fluids and/or small magmatic intrusions (hornblendite and clinopyroxenite sills/dikes) or partial melting [cf., *Matthews,* 1986; *Wever and Meissner,* 1987; *Vanderhaege and Teyssier,* 1997]. A decreased thickness of seismogenic (brittle) upper crust and repeated occurrence of **earthquake swarms** are observed above the Moho updoming and the local converters in the subcrustal mantle [*Horálek et al.,* 2000b, *this study*], which can be interpreted as rheological effects related to CO_2-dominated fluids. "Secondary phases" are observed in some local NW-Bohemia seismograms [*Boušková et al.*, 2003], which may originate at short distances from the hypocentres and are possibly caused by **spot-like low velocity zones** at the base of the upper crust filled with fluids.

The compilation of all results of previous and this studies indicates a systematic mantle/crust coupling maybe by the emplacement of mafic magmas near the base of the continental crust beneath the western Eger Rift. From bottom to top the following sub-processes can be distinguished (Figure D.2):

(1) release of CO_2-dominated fluid/magma from isolated crystallizing melt-reservoirs and/or metasomatic reactions in the depth range of 60 to 30 km; (2) active Moho updoming from about 31 to 27 km caused by thinning of the ductile lower crust at low angle shear zones as a consequence of magma/fluid/heat transport; (3) intrusion of alkaline melts into the lower crust forming dikes and sills (hornblendites, clinopyroxenites); (4) separation of CO_2 from such melts at 29 to 21 km depths and channel-like CO_2 transport through the crust; (5) occurrence of fluid triggered seismicity (earthquake swarms) in the depth range of 15 to 6 km which is caused by high pore fluid pressure in local captured upper crustal environment; (6) permeability of the upper crust beneath the area under investigation enable high permanent CO_2 transport through the upper crust.

This process is known under the term "magmatic underplating" in literature [*Furlong and Fountain*, 1986; *Griffin and O'Reilly,* 1987; *Cox,* 1993]. Geological, geophysical, and geochemical evidence suggest that magmatic underplating in extensional tectonic regimes is a first order process in the formation, growth, and modification of the oceanic and continental crust [cf., *Griffin and O'Reilly,* 1987; *O´Nions and Oxburgh*, 1988; *Jarchow et al.*, 1993; *Hansteen et al.,* 1998; *Grevemeyer and Flueh*, 2000; *Sachs and Hansteen,* 2000]. Seismic detecting of active magmatic underplating is clearly illustrated by the mid-ocean ridge magma additions [e.g., *Detrick et al.*, 1987; *Garmany*, 1989; *Caress et al.*, 1995]. Examples from the continental crust are rare in the literature [*Jarchow et al.*, 1993].

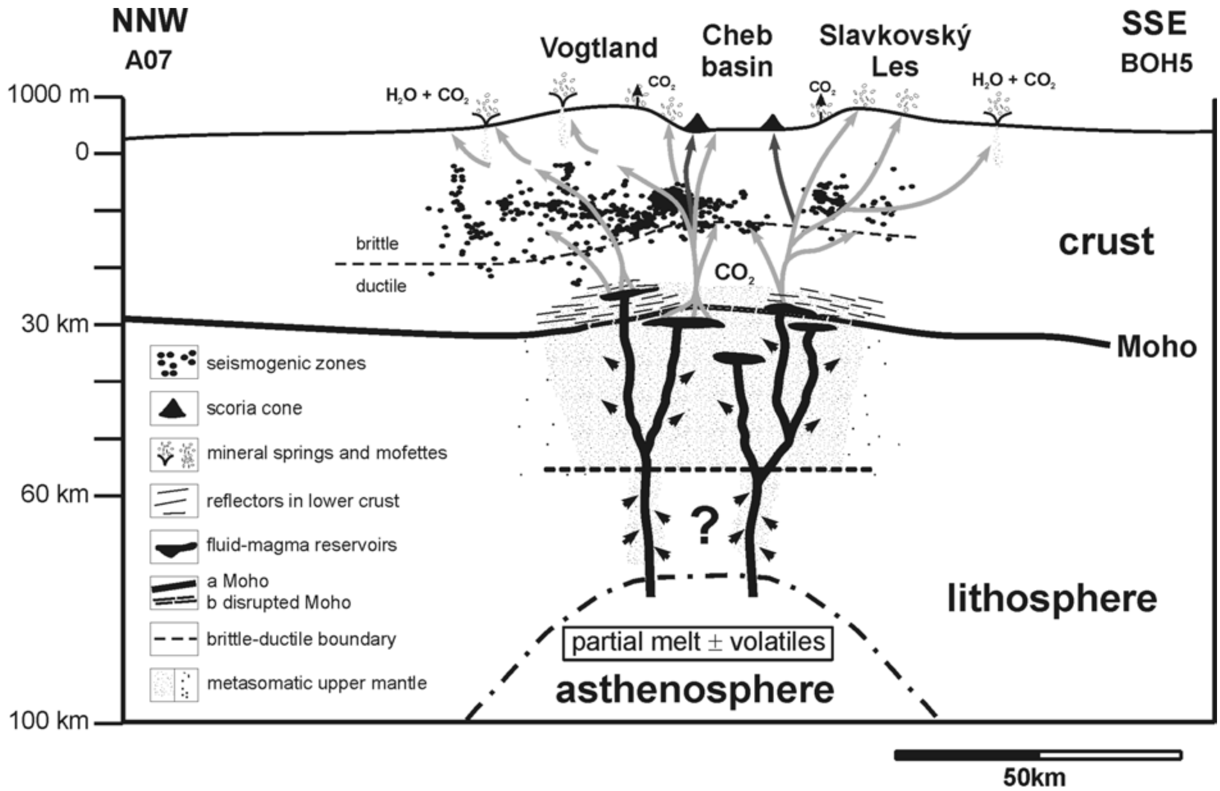

Figure D.2
Cartoon illustrating the asthenosphere-lithosphere interaction in the Vogtland/NW-Bohemia region.
The results of former studies [*Trappe and Wever,* 1990; *Tomek et al.,* 1997; *Vrána et al.,* 1997;*Babuška and Plomerová,* 2001; *Weinlich et al.,* 1999, 2003; *Horálek et al.,* 2000; *Bräuer et al.,* 2003, 2004] and the seismic and petrological results of this study were compiled. Black channels mark uprising CO_2 dissolved in melts; grey channels mark the CO_2/fluid transport through crust.
Observed converted phases at 6 seconds delay time might be caused by a thin low-velocity layer at the base of the seismogenic zone or at the base of a zone in the upper mantle with reduced seismic velocities. Reduced delay times of weak or lacking Moho conversions beneath the western Eger Rift points to overprinting of the crust-mantle boundary by magmatic and tectonic processes. Increased reflectivity within the lower crust and reduced thickness of the brittle upper crust possibly indicate that the discussed processes also affect the lower crust. Most of the seismic swarm activity is concentrated under the Vogtland area, whereas very little activity was detected in the other high CO_2 discharge zone in the Slavkovský Les area. This could be caused by the local crustal geology (Vogtland: interbedding of metasediments and metabasites / permeability barriers in seismogenic zones [*Bräuer et al.,* 2003]; Slavkovský Les: block of metabasites + granites) or differences in the local stress field.